

Modeling and Thermal Analysis of a CCP Collector System Based on Fractal Architecture: Receiver Proposal

Angélica Palacios¹, Darío Amaya^{2,*}, Olga Ramos³

¹u1801712@unimilitar.edu.co, Universidad Militar Nueva Granada, Colombia

²dario.amaya@unimilitar.edu.co, Universidad Militar Nueva Granada, Colombia

³olga.ramos@unimilitar.edu.co, Universidad Militar Nueva Granada, Colombia

Abstract. Solar concentrator technology has been researched in different fields in order to enhance efficiency and energy storage of these systems. Some changes in fluid and numerous components of the collectors have been proposed in recent years. In this context, this paper presents results associated to the modeling and thermal analysis of a concentrating system based on parabolic through collector with receiver pipe, designed with fractal geometry with the aim of improve system heat transfer. Founded on thermal modeling of heat transfer phenomena as radiation, convection and conduction, physical and mathematical relations between fractal geometrical parameters and transfer heat coefficient were established to find the influence of a chaotic structure on thermal behavior. Proposed designs were simulated through Solid works® Flow Simulation tool. Was possible obtain maximum temperatures in air with fractal and cylindrical pipes of 89°C, 86°C y 81°C respectively. The gap between fractal geometry results and cylindrical geometry is 10°C around.

1 Introduction

Within technology with high development in solar energy, we found first of all, photovoltaic and concentrating collectors. The last, count with a system of thermal energy storage, wherewith is possible improve the controlling capacity of the concentrating system output [1]. For the year 2050 it hopes that concentrating stations by parabolic cylindrical collectors (CCP), satisfices global demand in a 6%, [2]. At the same, energy system will benefit by this kind of technology, contaminate emissions decrease, electrical trade reliability and renewable energies, will be evident across de world. [3]–[6]. Within advantages it's found accessible cost, high concentration, thermal storage wherewith the system works full power, even if solar radiation is not available for hours [7].

Some studies and researches globally, about solar collection systems by parabolic cylindrical collectors, are related with heat transfer enhancement in receiver pipe under different guidelines, [8]–[10]. Some of them directly interact with pipe and other ones with transfer fluid. In the last one, Nano-fluids and Nano-particles concepts are involves in collector thermal efficiency, [11]–[13]. Although presently this kind of fluids are not applied in CCP stations, use of them involve specific requirements in hydraulic elements as pumps, valves, connection pipes, among others, [14]. Nano-fluids potential has been experimented in [15], where heat transfer with forced convection was studied, inside the receiver of a parabolic cylindrical collector. From there,

was possible identify a 28% increase of thermal coefficient with Al₂O₃ – H₂O combination and a 35% increase with CuO- H₂O combination regard to pure water.

Furthermore, receiver pipe modification has been achieved in different researches, some works present mechanical design where pipe has inside fin kind incrustations. At the same, receiver size has been studied, with the purpose of enhancement system heat transfer, [16], with the thermal resistance decrease, turbulence intensity increase and increase of effective thermal conductivity. As presented in [17], [18], where thermal and thermodynamic efficiency of a CCP was analyzed with a perforated plate, geometrical parameters related to the plate as slope angle, were modified in the research, a 8% increase was obtained in system efficiency.

Within modifications developed in receiver to enhance the transference, is proposed convex pipes, symmetrical and asymmetrical. In papers as [19], [20], was possible obtain varied in efficiency with Reynolds number increase in some geometrical parameters. Finally, a 135% increase was obtained in heat transfer for a symmetrical geometry and 148% increase for asymmetrical geometry. Use of fractal geometry has been developed in some researches to enhance flow conditions. In [21] modelling and experimental study, was developed about flow distribution and heat transfer of a system conformed with hollow fibers in a fractal array structure. Likewise, friction factor and irregularity according to fractal dimension was studied. Wherewith

* Corresponding author: dario.amaya@unimilitar.edu.co

results it's found, that a minor fractal dimension the uniformity in flow distribution decrease.

This paper present the results obtained with a modelling and thermal analyses of a concentrating system by parabolic cylindrical collector with a pipe receiver, designed based on fractal geometries. With the purpose of enhancement in heat transfer modifying hydraulic diameter and transversal area where heat fluid flow.

2 Methods

2.1 Solar Resource

A high quantity of energy equivalent to $1.74 \times 10^7 W$, is radiated by Sun to Earth atmosphere. However, this energy don't achieved in a 100% the surface, is attenuated by reflection, absorption and dispersion phenomena involved in chemistry components which conform air planet. Thus, almost 51% of radiated energy achieved the surface, despite the percentage represent a high energy [22], [23]. On a parabolic cylindrical collector, as shown in Figure 1, radiated energy by Sun and focused on Earth is concentrated on an area, known as aperture area.

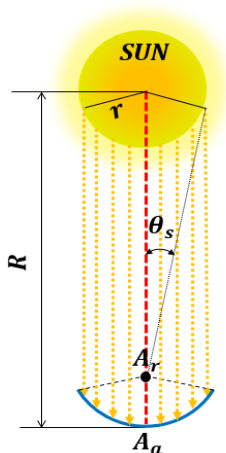


Figure 1. Solar-collector relation.

2.2 CCP Construction by Parabolic Geometry

A construction of parabolic cylindrical collector, is based on parabolic equation relation (Eq.(1)), which parable aperture depends of the height and focal distance.

$$X^2 = 4fY \quad (1)$$

Under rays concentrating theory as of parabolic surface to receiver pipe, when focusing rays by reflection in parable geometry of focal distance. Related parameters in concentrating CCP theory, are illustrated in Figure 2.

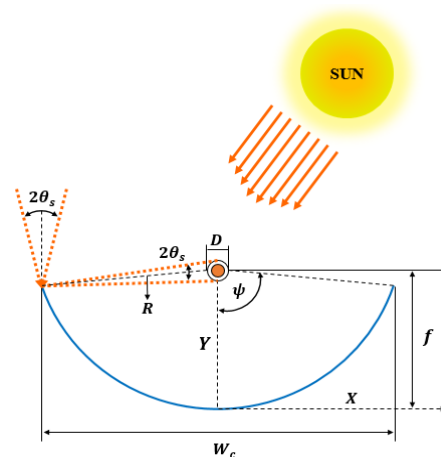


Figure 2. Parabolic Cylindrical Collector geometry.

To calculated keys parameters of collector design, as receiver diameter (D), parable width (W_c), focal distance (f) and finally concentration ratio (C_n) are stablish geometrical relations presented down below. Receiver diameter (Eq.(2)), is related with admissible incident angle ($\theta_s = 16^\circ$), through trigonometric association with distance between concentrating point [R] and parabolic surface.

$$D = 2 \times R \times \sin(\theta_s) \quad (2)$$

Similarly, the aperture width of parable is obtained with trigonometric relations, between rim angle and distance (R), as shown in (Eq.3).

$$\begin{aligned} W_c &= 2 \times R \times \sin(\psi) = \frac{4f \sin \psi}{1 + \cos \psi} \\ &= 4f \times \tan\left(\frac{\psi}{2}\right) \end{aligned} \quad (3)$$

Finally, concentrating ratio of a parabolic cylindrical collector (C_n), is realted between aperture area of collector (A_a) and focus area o receiver (A_r). This parameter is described by (Eq.4).

$$C_n = \frac{A_a}{A_r} = \frac{W_c}{\pi D} \quad (4)$$

To obtain design parameters, a concentration factor was set of ($C_n = 10$) and a diameter of ($D = 0.0254$ m). Other surface and receiver dimensions are presented in Table 1.

Table 1 .CCP Dimensions

Surface Dimensions		
Parameter	Value	Unity
W_c	0.798	[m]
f	0.199	[m]
X_{max}	-0.4	[m]
Y_{max}	0.4	[m]
ψ	90	[°]
R	0.4	[m]
L_c	0.92	[m]
Receiver Dimensions		
D	0.0254	[m]
L_r	0.92	[m]

2.3 Proposed Design

Once conventional parabolic cylindrical collectors were analyzed, as well as enhancement elements to improve heat transfer. In this paper is proposed a design of a pipe based on fractal geometry with the purpose of enhance area and transfer coefficients. Pipe geometries are presented down below in Figure 3.

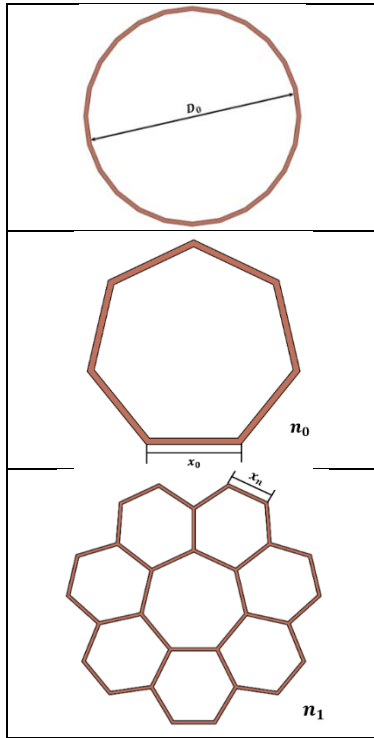


Figure 3. Receiver geometry.

Sides number (k_n) of fractal depends of initial value ($k_0 = 7$), in next iterations ($\{n_1, n_2, \dots, n_n\}$), the representation is given by (Eq.(5)). Geometry scale factor (f_s) consist in number of elements involve on geometry, ($n_0 f_{s=1}$). For next iterations factor can be defined as (Eq.(6)).

$$k_n = 3 \times k_{n-1} \tag{5}$$

$$f_s = \frac{k_n}{3} + 1 \tag{6}$$

Fractal geometry analysis on receiver thermal study is based on transfer area and the relation with convection coefficient, through hydraulic diameter ($D_{h[n]}$). The last depends of transversal area (A_t) and perimeter (P) of seven sides polygon (n) as (Eq.7).

$$D_{h[n]} = \frac{4 \times A_{[n]}}{P_{[n]}} \tag{7}$$

2.4 Study Conditions

CFD Model

Laminar model of Flow Simulation tool in SolidWorks software, Works with Navier Stokes equations [24],

where conservation of mass, momentum and energy laws are related on a cartesian coordinate system [25], [26]. These equations are presented down below [Eq.(8 - Eq.(10)].

$$\frac{\partial \rho}{\partial t} + \frac{\partial}{\partial x_i}(\rho u_i) = 0 \tag{8}$$

$$\frac{\partial \rho u_i}{\partial t} + \frac{\partial}{\partial x_j}(\rho u_i u_j) + \frac{\partial p}{\partial x_i} = \frac{\partial}{\partial x_j}(\tau_{ij} + \tau^R_{ij}) + S_i \tag{9}$$

$i = 1, 2, 3$

$$\frac{\partial \rho H}{\partial t} + \frac{\partial \rho u_i H}{\partial x_i} = \frac{\partial}{\partial x_i}(u_j(\tau_{ij} + \tau^R_{ij}) + q_i) + \frac{\partial p}{\partial t} - \tau^R_{ij} \frac{\partial u_i}{\partial x_j} + \rho \epsilon + S_i u_i + Q_H, H = h + \frac{u^2}{2} \tag{10}$$

3 Analysis and Results

Study results for each proposed receiver are presented independently. First is described outlet temperature in fluid and concentrator temperature increasing, with cylindrical pipe for each fluid (air, refrigerant and ethylene).

3.1 Cylindrical Receiver

Maximum temperature in air, refrigerant and ethylene inside of cylindrical pipe was 81.56°C, 83.79°C and 80.216°C respectively. The maximum delta of temperature was found in refrigerant as fluid, where initial temperature was increased around 62°C. The results are related in Table 2.

Table 2. Cylindrical Receiver

Fluid	Solid		Fluid	
	T_{max} [°C]	ΔT [°C]	T_{max} [°C]	ΔT [°C]
Air	81.57	59.76	81.57	59.75
R4010	83.79	61.97	83.79	61.97
Ethylene	80.22	58.39	80.21	58.39

Inside and outside temperature distribution of cylindrical pipe are shown in the image of Figure 4. Temperature vary between 64°C and 77°C on pipe zone, was the highest temperature on solid.

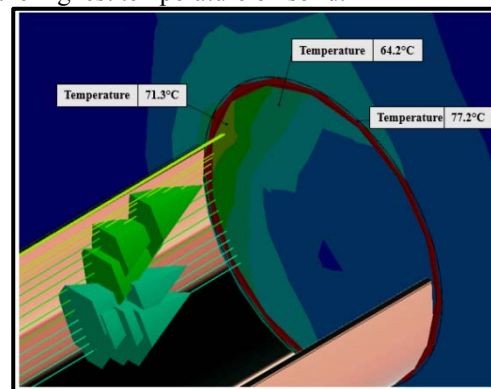


Figure 4. Thermal results of receiver with air.

Curves in Figure 5 present the temperature of each fluids inside cylindrical pipe. As shown refrigerant was the highest temperature followed by air and ethylene.

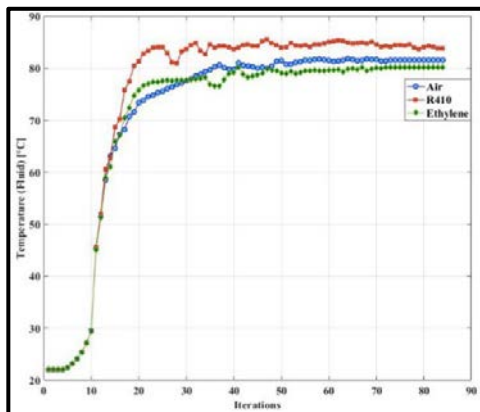


Figure 5. Thermal graph of cylindrical pipe.

3.2 Fractal n_0 Receiver

Maximum temperature and delta temperatures obtained on receiver and each analyzed fluids are presented on Table 3. Highest temperature in receiver was 86.54°C with air as fluid, while refrigerant achieved a maximum temperature of 80.95°C, finally ethylene present a temperature of 6.57°C less than the maximum obtained. Similar variation to the calculated with refrigerant as fluid.

Table 3. Receiver-Fractal N0

Fluid	Solid		Fluid	
	T_{max} [°C]	ΔT [°C]	T_{max} [°C]	ΔT [°C]
Air	86.55	63.87	86.55	64.36
R4010	80.96	58,91	80.96	59.06
Ethylene	79.97	58	79.97	58.34

Figure 6 shows temperature distribution on pipe and fluid which flow through receiver. The highest temperature on this section was in pipe surface with a 84.46°C, furthermore air achieved a temperature of 76.67°C, while envirement remain in 22°C.

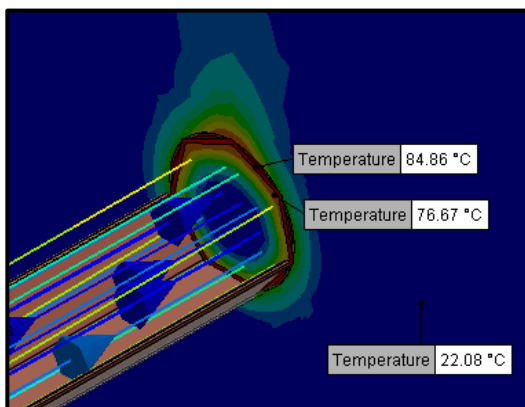


Figure 6. Thermal results of receiver with air.

As shown in graph of Figure 7, air was the fluid with the highest temperature, followed by refrigerant and

ethylene. Each of the fluids present a temperature increase of 64.35°C, 59.06°C y 58.33°C respectively.

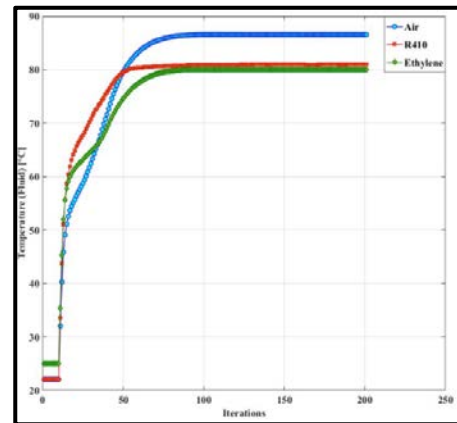


Figure 7. Thermal graph of pipe n0.

3.3 Fractal n_1 Receiver

Obtained results in the analysis of solar concentrator with Fractal pipe n_1 , are describes in Table 4. Receiver temperature and different fluids are presented in this table. In contrast to receiver n_0 fluid which system achieved the highest temperature in receiver n_1 was refrigerant with a temperature of 88.84°C, however difference between air is only 0.19°C, thus values are really nearby to compare. Furthermore, with ethylene the solid achieved a maximum temperature of 83.74°C and a delta of 62.68°C.

Table 4. Receiver-Fractal N1

Fluid	Solid		Fluid	
	T_{max} [°C]	ΔT [°C]	T_{max} [°C]	ΔT [°C]
Air	88.65	67.47	88.66	67.65
R4010	88.84	67.76	88.85	67.76
Ethylene	83.75	62.69	83.75	62.69

Fluid temperature (R410) inside the fractal pipe n_1 , is ilustrated in Figure 8. Through the image is possible evidence the temperature distribution from the inside to exterior pipe, where areas with a maximum heat concentration find in receiver pipe.

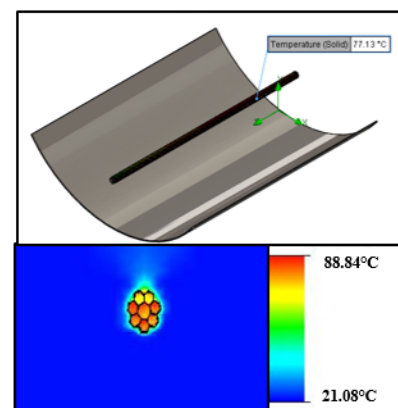


Figure 8. Receiver n_1 thermal results with R410.

Finally, graph in Figure 9 illustrated the temperature in different fluids (air, refrigerant and ethylene) studied in geometry of receiver n_1 . Based on the figure is possible to identify closeness between thermal performance in air and refrigerant, while ethylene show a difference regard to the others fluids around 5°C.

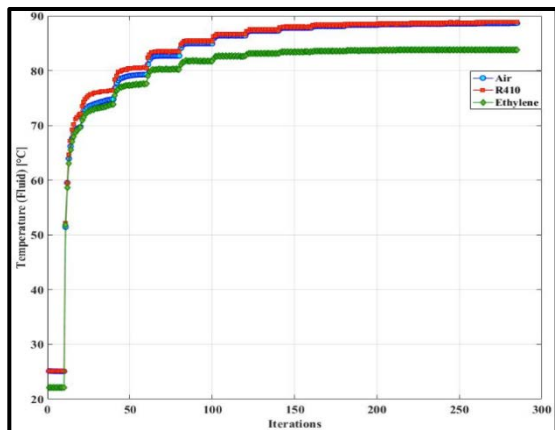


Figure 9. Thermal graph of pipe n_1 .

As was evident the geometry with the highest temperature in fluid was the concentrator with fractal receiver n_1 , achieved a maximum value of 88.84°C with refrigerant. The system with the lowest temperature both fluid and solid was the concentrator with cylindrical receiver, which obtain a maximum temperature of 83.79°C with refrigerant as fluid. Table 5 present the results unified for analyzed systems.

Table 5. Receiver results.

Pipe	Fluid	T max [°C]
Cylindrical	Air	81.57
	R410	83.79
	Ethylene	80.21
Fractal n_0	Air	86.55
	R410	80.96
	Ethylene	79.97
Fractal n_1	Air	88.66
	R410	88.85
	Ethylene	83.75

4 Conclusions

Different geometries for pipe receiver of a parabolic cylindrical collector were studied in this work. Both conventional cylindrical pipe, heptagonal pipe and next iteration of lineal fractal, general heat transfer coefficient or convection coefficient, vary according to hydraulic diameter and transfer area, which are related with Nusselt and Reynolds number, by reducing in each fractal iteration the geometry diameter is increase the transfer heat.

The fractal tube n_1 was the system that reached the highest temperature in simulation, under the same conditions and the different fluids used in the study. The maximum temperature reached in this tube was approximately 89°C with an increase in the initial

temperature of 68°C, with R410 refrigerant as the transfer fluid. Furthermore, the conventional cylindrical pipe reached the lowest temperatures of the study with an average of 81.85°C in the fluids.

For the cylindrical geometry and the fractal n_1 in the receiver pipe, the fluid with the best thermal behavior was the air, while the fractal geometry n_0 presented better results with air. The difference between this and R410 refrigerant was 6°C, with a maximum temperature in the fluid of 86.55°C. In turn, it was possible to identify that the difference in the results obtained by the fractal geometries was approximately 2°C, while the difference with the cylindrical geometry was approximately 10°C.

Acknowledgment

The authors would like to thank the Nueva Granada Military University research center for financing this work (research project IMP-ING-2656, 2019).

References

1. S. Zhao Y. Fang, and Z. Wei, “Stochastic optimal dispatch of integrating concentrating solar power plants with wind farms,” *Int. J. Electr. Power Energy Syst.*, vol. **109**, pp. 575–583, (2019).
2. S. Izquierdo, C. Montanes, C. Dopazo, and N. Fueyo, “Analysis of CSP plants for the definition of energy policies: The influence on electricity cost of solar multiples, capacity factors and energy storage,” *Energy Policy*, vol. **38**, no. 10, pp. 6215–6221, (2010).
3. K. Dallmer-Zerbe, M. Bucher, A. Ulbig, and G. Andersson, “Assessment of capacity factor and dispatch flexibility of concentrated solar power units,” in *IEEE Grenoble Conference*, (2013), pp. 1–6.
4. P. Denholm and M. Hummon, “Simulating the value of concentrating solar power with thermal energy storage in a production cost model,” *Contract*, vol. **715**, no. 6, pp. 1–4, (2013).
5. S. Madaeni, R. Sioshansi, and P. Denholm, “Estimating the capacity value of concentrating solar power plants with thermal energy storage: A case study of the southwestern United States,” *IEEE Trans. Power Syst.*, vol. **28**, no. 2, pp. 1205–1215, (2013).
6. G. He, Q. Chen, C. Kang, and Q. Xia, “Optimal offering strategy for concentrating solar power plants in joint energy, reserve and regulation markets,” *IEEE Trans. Sustain. Energy*, vol. **3**, no. 3, pp. 1245–1254, 7AD.
7. R. Sioshansi and P. Denholm, “The value of concentrating solar power and thermal energy storage,” *IEEE Trans. Sustain. Energy*, vol. **1**, no. 3, pp. 173–183, (2010).
8. H. Ghaebi, T. Parikhani, H. Rostamzadeh, and B. Farhang, “Thermodynamic and thermoeconomic analysis and optimization of a novel combined cooling andz power (CCP) cycle by integrating of

- ejector refrigeration and,” *Energy*, vol. **139**, pp. 262–276, (2017).
9. H. Rostamzadeh, M. Ebadollahi, H. Ghaebi, M. Amidpour, and R. Kheiri, “Energy and exergy analysis of novel combined cooling and power (CCP) cycles,” *Appl. Therm. Eng.*, vol. **124**, pp. 152–169, (2017).
 10. M. Pan, I. Bulatov, and R. Smith, “Improving heat recovery in retrofitting heat exchanger networks with heat transfer intensification, pressure drop constraint and fouling mitigation,” *Appl. Energy*, vol. 161, pp. 611–626, 2016.
 11. B. Balakin, O. Zhdaneev, A. Kosinska, and K. Kutsenko, “Direct absorption solar collector with magnetic nanofluid: CFD model and parametric analysis,” *Renew. Energy*, vol. **136**, pp. 23–32, (2019).
 12. M. Dehaj and M. Cells, “Experimental investigation of heat pipe solar collector using MgO nanofluids,” *Sol. Energy Mater. Sol. Cells*, vol. **191**, (2019).
 13. K. Farhana et al., “Improvement in the performance of solar collectors with nanofluids—A state-of-the-art review,” *Nano-Structures & Nano-Objects*, vol. **18**, (2019).
 14. A. Kasaeian, A. Eshghi, and M. Sameti, “A review on the applications of nanofluids in solar energy systems,” *Renew. Sustain. Energy Rev.*, vol. **45**, pp. 584–598, (2015).
 15. S. Ghasemi and A. Ranjbar, “Thermal performance analysis of solar parabolic trough collector using nanofluid as working fluid: a CFD modelling study,” *J. Mol. Liq.*, vol. **222**, pp. 159–166, (2016).
 16. E. Baysal, A. R. Dal, and N. Şahin, “Investigation of heat transfer enhancement in a new type heat exchanger using solar parabolic trough systems,” *Int. J. Hydrogen Energy*, vol. **40**, no. 44, pp. 15254–15266, Nov. (2015).
 17. A. Mwesigye, T. Bello-Ochende, and J. P. Meyer, “Multi-objective and thermodynamic optimisation of a parabolic trough receiver with perforated plate inserts,” *Appl. Therm. Eng.*, vol. **77**, pp. 42–56, (2015).
 18. A. Mwesigye, T. Bello-Ochende, and J. P. Meyer, “Heat transfer and thermodynamic performance of a parabolic trough receiver with centrally placed perforated plate inserts,” *Appl. Energy*, vol. **136**, pp. 989–1003, (2014).
 19. W. Fuqiang, L. Qingzhi, H. Huaizhi, and T. Jianyu, “Parabolic trough receiver with corrugated tube for improving heat transfer and thermal deformation characteristics,” *Appl. Energy*, vol. **164**, pp. 411–424, (2016).
 20. W. Fuqiang, T. Zhexiang, G. Xiangtao, T. Jianyu, H. Huaizhi, and L. Bingxi, “Heat transfer performance enhancement and thermal strain restraint of tube receiver for parabolic trough solar collector by using asymmetric outward convex,” *Energy*, vol. **114**, pp. 275–292, (2016).
 21. L. Z. Zhang, “Heat and mass transfer in a randomly packed hollow fiber membrane module: a fractal model approach,” *Int. J. Heat Mass Transf.*, vol. **54**, pp. 13–14, (2011).
 22. T. Li, R. Wang, J. Kiplagat, and Y. Kang, “Performance analysis of an integrated energy storage and energy upgrade thermochemical solid–gas sorption system for seasonal storage of solar thermal,” *Energy*, vol. **50**, pp. 454–467, (2013).
 23. X. Meng, X. Xia, C. Sun, and X. Hou, “Adjustment, error analysis and modular strategy for Space Solar Power Station,” *Energy Convers. Manag.*, vol. **85**, pp. 292–301, (2014).
 24. X. J. Yang, D. Baleanu, and J. A. Tenreiro Machado, “Systems of Navier-Stokes equations on Cantor sets,” *Math. Probl. Eng.*, (2013).
 25. G. Galdi, “An introduction to the mathematical theory of the Navier-Stokes equations: Steady-state problems,” (2011).
 26. J. Ferziger and M. Peric, *Computational methods for fluid dynamics*. (2012).